J|A|C|S
ARTICLES
Published on Web 03/30/2006

Microbead Chemical Switches: An Approach to Detection of Reactive Organophosphate Chemical Warfare Agent Vapors

Sandra Bencic-Nagale, Tamar Sternfeld, and David R. Walt*

Contribution from the Department of Chemistry, Tufts University, Medford, Massachusetts 02155

Received October 17, 2005; E-mail: david.walt@tufts.edu

Abstract: In this article, we describe the preparation and application of microbeads that exhibit a "turn on" fluorescence response within seconds of exposure to diethyl chlorophosphate (DCP) vapor. This sensing approach is modeled after the mechanism for acetylcholinesterase enzyme activity inhibition and uses a specific and irreversible reaction between phosphoryl halides and a fluorescent indicator. The microbeads are fabricated by adsorbing fluoresceinamine (FLA) onto carboxylate-functionalized polymer microbeads coated with poly(2-vinylpyridine) (PVP). When the microbeads are subjected to DCP vapor, the conversion of FLA into a phosphoramide causes a rapid and intense fluorescence increase. The PVP layer provides a high density of proton-accepting pyridine nitrogen sites that neutralize the HCl released during the reaction, thereby maintaining high product fluorescence, even after vapor exposure. No significant response is observed when the microbeads are subjected to other nerve agent simulants, a mustard gas simulant, and volatile organics. The size, sensitivity, and subsecond response of these microbeads make them suitable for nerve agent vapor detection and inclusion into microbead sensor arrays.

Introduction

The threat of chemical attack with aqueous or gas-phase organophosphates has been the motivation for extensive research in recent years.[1−14] Many existing sensing methods (e.g., electrochemical,[1−5] surface acoustic wave,[6,7] colorimetric,[8] fluorescence-[9] and luminescence-based[10]) target fast, portable, and inexpensive recognition. Sensors used to detect vapor phase nerve agent release in populated areas rely on specificity and subsecond response to ensure that the released vapor is always accurately identified.[6,9] Existing organophosphate vapor sensors are based on materials (e.g., fluorescent indicators,[9] polymers,[7,12] metal oxides,[13,14] and gold nanoparticles[8]) developed for fast recognition of a specific organophosphate or other functional groups. Materials research has thus far focused mostly on discovering chemical entities that enable chemical warfare recognition, with less effort spent on sensor miniaturization and integration. As a consequence, the present sensors have not been specifically designed to fit within existing multiplex vapor detection systems, such as sensor arrays, including electronic noses. Integration into such arrays is important, as array platforms contain multiple sensor types that can detect a wide spectrum of harmful vapors, with nerve agents representing only a small percentage of these vapors. The ability to detect toxic chemical agents is facilitated by sensors that can identify these agents in a variety of contexts, including backgrounds containing high concentrations of nontoxic chemicals.

The electronic nose system developed in our laboratory[15,16] is a fluorescence-based array containing thousands of individually optically addressable micrometer-scale vapor sensors. Each array is prepared by loading 3−5-μm-diameter microbead sensors into 4.5-μm-diameter wells, etched into a fiber-optic bundle. This technology is advantageous for multiplexing and accommodating newly developed microsensors for a number of reasons: microbead batches are highly reproducible and inexpensive to fabricate, the sensor library may be expanded at any point in time, individually addressable multiple replicates of different microbead sensor types are accommodated on a highly dense array platform, and the arrays respond to vapors in subsecond times.[15,17−19] Previously, we developed cross-reactive vapor sensing arrays, in which each sensor type is cross-

(1) Lin, Y.; Lu, F.; Wang, J. *Electroanalysis* **2004**, *16*, 145−149.
(2) Zhou, Y.; Yu, B.; Shiu, E.; Levon, K. *Anal. Chem.* **2004**, *76*, 2689−2693.
(3) Yu, D.; Volponi, J.; Chhabra, S.; Brinker, C. J.; Mulchandani, A.; Singh, A. K. *Biosens. Bioelectron.* **2005**, *20*, 1433−1437.
(4) Anitha, K.; Mohan, S. V.; Reddy, S. J. *Biosens. Bioelectron.* **2004**, *20*, 848−856.
(5) Simonian, A. L.; Grimsley, J. K.; Flounders, A. W.; Schoeniger, J. S.; Cheng, T. C.; DeFrank, J. J.; Wild, J. R. *Anal. Chim. Acta* **2001**, *442*, 15−23.
(6) Yang, Y.; Ji, H.-F.; Thundat, T. *J. Am. Chem. Soc.* **2003**, *125*, 1124−1125.
(7) Hartmann-Thompson, C.; Hu, J.; Kaganove, S. N.; Keinath, S. E.; Keeley, D. L.; Dvornic, P. R. *Chem. Mater.* **2004**, *16*, 5357−5364.
(8) Pavlov, V.; Xiao, Y.; Willner, I. *Nano Lett.* **2005**, *5*, 649−653.
(9) Zhang, S.-W.; Swager, T. M. *J. Am. Chem. Soc.* **2003**, *125*, 3420−3421.
(10) Jenkins, A. L.; Uy, O. M.; Murray, G. M. *Anal. Chem.* **1999**, *71*, 373−378.
(11) Jenkins, A. L.; Yin, R.; Jensen, J. L.; Durst, H. D. *Polym. Mater. Sci. Eng.* **2001**, *84*, 76−77.
(12) Levitsky, I.; Krivoshlykov, S. G.; Grate, J. W. *Anal. Chem.* **2001**, *73*, 3441−3448.
(13) Utriainen, M.; Karpanoja, E.; Paakkanen, H. *Sens. Actuators, B* **2003**, *B93*, 17−24.
(14) Tomchenko, A.; Harmer, G. P.; Marquis, B. *Chem. Sens.* **2004**, *20*, 34−35.
(15) Dickinson, T. A.; Michael, K. L.; Kauer, J. S.; Walt, D. R. *Anal. Chem.* **1999**, *71*, 2192−2198.
(16) Dickinson, T. A.; White, J.; Kauer, J. S.; Walt, D. R. *Nature (London)* **1996**, *382*, 697−700.
(17) Albert, K. J.; Walt, D. R. *Anal. Chem.* **2000**, *72*, 1947−1955.

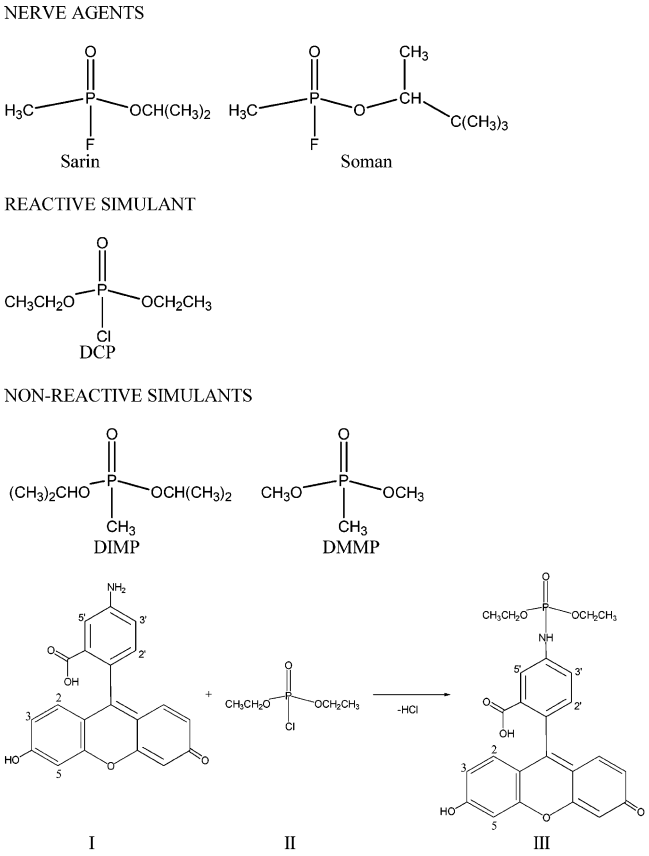

Figure 1. Structures of nerve agents and the target compounds utilized in this study and reaction schematic of FLPA formation (III) upon reaction between the probe (I) and DCP (II).

reactive and responds to many vapors.[18] Although cross-reactive sensors can respond reversibly hundreds of times,[20] there is often a delay in identifying the vapor because the data must be evaluated using time-consuming pattern recognition algorithms. Moreover, difficult vapor discrimination tasks, such as differentiation between nerve agents and their less harmful simulants, may prolong the data processing time because challenging vapor queries often require the extraction of extensive amounts of information from the sensor responses. Vapor detection tasks necessitating immediate answers should not employ sensors that require such lengthy data processing; for such tasks, specific probes are preferable to cross-reactive sensors. Although specific probes that react with the target vapor irreversibly present a drawback as they may be used only a single time, their rapid response speed and specificity overshadow the disadvantage in having to replace the array after a vapor release has occurred. In such cases, the value of having a rapid responding probe for a rare event makes replacement acceptable as long as the chemistry is designed to provide zero false positive results.

We have developed nerve-agent-reactive microbead probes (e.g., for Sarin and Soman, Figure 1) for integration into our existing microarray platform. Because nerve agents possess reactive groups that inhibit acetylcholinesterase by covalent modification of its active site, our goal was to prepare nerve agent probes that only respond to reactive molecules including simulants such as DCP (Figure 1), an acetylcholinesterase inhibitor with effects similar to the nerve agents. Ideally, the probes would be nonresponsive to less harmful compounds that lack a reactive acyl or phosphoryl halide functionality (e.g., simulants dimethyl methylphosphonate (DMMP) and diisopropyl methylphosphonate (DIMP)). Many previously developed sensors are not sufficiently specific as they detect both reactive and nonreactive simulants. The Swager group recently developed novel probe compounds that overcome the lack of specificity common in other phosphonate warfare sensors as they react only with phosphoryl halides.[9] Their probe compounds are designed to detect acetylcholinesterase inhibitor organophosphates when they form fluorescent esters upon reaction with phosphoryl halides. In addition to specificity, sensitivity, and fast response, these probes are advantageous due to their turn-on behavior upon binding the target analyte. Turn-on sensors are more reliable than turn-off sensors because their signal arises from a low background.[21,22] False positives are rarely observed with turn-on sensors because, unlike turn-off sensors, high background intensity and photobleaching minimally affect their overall response. Turn-on sensor properties have also been demonstrated with rhodamine derivatives that fluoresce upon selective reaction with Hg^{2+} ions.[23]

In this article, we present an alternative fluorescent indicator with the desired reactivity and fluorescence properties. Fluoresceinamine (FLA), a commercially available fluorescent dye with reactivity for phosphoryl halides, is used to fabricate microbead sensors. Previous studies in our laboratory demonstrated that FLA could be used as a turn-on fluorescent indicator; when FLA's amine group reacts with acyl and phosphoryl halides, its quantum yield increases dramatically.[24,25] This mechanism was observed as a 50-fold fluorescence increase (relative to the amine) upon reaction of FLA with acryloyl chloride. Thus, FLA (Figure 1, I) is a natural choice for a microbead phosphoryl halide probe because its reactivity is well established and the requisite form for sensing is commercially available. The size and geometry of the microbead sensors described here allow their inclusion into populations containing various cross-reactive sensors, such that they can be positioned on a microwell array and used as an early warning sentinel in conjunction with the optical electronic nose. The FLA microbead probes respond within seconds of exposure to DCP, and their fluorescence signal increase is stable. These rapid and specific microbead probes show the potential to confidently alert a sudden release of nerve agents in real time.

Experimental Section

Materials and Instrumental Setup. Fluoresceinamine (isomer I), ethanol, potassium phosphate monobasic solution (1 M), potassium phosphate dibasic solution (1 M), hydrochloric acid, sodium hydroxide, acryloyl chloride, diethyl chlorophosphate, dimethyl methylphosphonate, and poly(2-vinylpyridine) (PVP) (secondary standard; M_w = 37 500, M_n = 35 000) were purchased from Aldrich (Milwaukee, WI)

(18) Albert, K. J.; Lewis, N. S.; Schauer, C. L.; Sotzing, G. A.; Stitzel, S. E.; Vaid, T. P.; Walt, D. R. *Chem. Rev.* **2000**, *100*, 2595−2626.
(19) Stitzel, S. E.; Cowen, L. J.; Albert, K. J.; Walt, D. R. *Anal. Chem.* **2001**, *73*, 5266−5271.
(20) Bencic-Nagale, S.; Walt, D. R. *Anal. Chem.* **2005**, *77*, 6155−6162.
(21) Mortellaro, M. A.; Nocera, D. G. *CHEMTECH* **1996**, *26*, 17−23.
(22) Fan, C.; Plaxco, K. W.; Heeger, A. J. *Proc. Natl. Acad. Sci. U.S.A.* **2003**, *100*, 9134−9137.
(23) Yang, Y.-K.; Yook, K.-J.; Tae, J. *J. Am. Chem. Soc.* **2005**, *127*, 16760−16761.
(24) Munkholm, C.; Walt, D. R.; Milanovich, F. P.; Klainer, S. M. *Anal. Chem.* **1986**, *58*, 1427−1430.
(25) Munkholm, C.; Parkinson, D. R.; Walt, D. R. *J. Am. Chem. Soc.* **1990**, *112*, 2608−2612.

and used as received. Diisopropyl methylphosphonate (DIMP) was purchased from Lancaster Synthesis (Lancashire, UK). Silica microbeads (3-μm diameter) were retrieved from a Luna Silica(2) liquid chromatography column (Phenomenex, Torrance, CA), washed with toluene, and dried at 60 °C overnight. Polystyrene (PS05N, 2.93-μm diameter, water suspension, 10% solids) and carboxylate-modified polystyrene (PC05N, 3.20-μm diameter, water suspension, 10% solids) microbead suspensions in water were purchased from Bangs Laboratories (Fishers, IN). Glass coverslips (30-mm diameter) were purchased from ProSciTech (Queensland, Australia). Optical fiber bundles with 4.5-μm-diameter wells, used in the preparation of microbead arrays, were purchased from Illumina, Inc. (San Diego, CA).

^{1}H NMR spectra were recorded on a Bruker AM-300 spectrometer. Chemical shifts were measured relative to the solvent peaks (DMSO-d_6 2.50 ppm relative to TMS). ESI-MS spectra were acquired with a Finnigan LTQ spectrometer (Thermo Electron Corporation, Waltham, MA). Fluorescence emission spectra were acquired with a SpectraMax Gemini microplate spectrofluorometer (Sunnyvale, CA). Fluorescence measurements in solution and vapor responses were acquired with a fluorescence imaging system, slightly modified with respect to a previously described one.[19] In brief, the system comprised a BX Olympus horizontal microscope (Melville, NY), automated excitation and emission filter wheels, a 75 W xenon excitation source (Ludl, Hawthorne, NY), and a Sensicam QE (1376 × 1040 pixel) CCD Camera (Cooke Corp., Auburn Hills, MI). Additional optics included a 20× objective, 1.6× and 0.5× optical lenses, and several neutral density filters. 4 × 4 binning was employed in all measurements.

Synthesis of Fluorescein Phosphoramide. A dry system that consisted of a reaction flask connected to a condenser with a $CaCl_2$-filled tube was used for the synthesis of the phosphoramide product. Fluoresceinamine (50 mg; 0.14 mmol) was first dissolved in 1.5 mL of acetone to form a yellow solution. The solution color changed to orange upon addition of diethyl chlorophosphate (25 μL; 0.17 mmol). The reaction mixture was stirred at room temperature for 48 h until the fluorescein phosphoramide (FLPA) precipitated. Subsequent vacuum filtration and multiple acetone rinses were followed by evaporation to recover the product (orange powder), which was characterized by ^{1}H NMR and MS: ^{1}H NMR δ 1.26 (t, 6 H, J = 7.02 Hz, CH_3), 4.07 (m, 4 H, OCH_2), 6.57 (m, 4 H, H_2, H_3), 6.66 (s, 2 H, H_5), 7.12 (d, 1 H, J = 8.5 Hz, $H_{2'}$), 7.4 (dd, 1 H, J_1 = 8.16 Hz, J_2 = 1.9 Hz, $H_{3'}$), 7.51 (d, 1 H, J = 1.7 Hz, $H_{5'}$), 8.61 (d, 1 H, J = 9.10, NH), 10.1 (br, 1 H, OH); exact mass calcd for $C_{24}H_{22}NO_8P + H^+$: 484.12, found: 484.06.

Preparation of Silica−FLA Beads. Silica (S) microbeads (15 mg) were mixed with 1.5 mL of 1 mM fluoresceinamine in 0.05 M phosphate buffer (pH 7.5) for 2 h, filtered, washed with buffer, and dried at 60 °C overnight.

Preparation of Polymer−FLA Beads. Aliquots (200 μL) of polystyrene microbeads (PS) and vinyl carboxylic acid/polystyrene copolymer microbeads with carboxylate surface groups (PSC) were washed separately three times with 0.5 mL of ethanol by centrifugation and removal of the supernatant. The microbeads were resuspended in 0.5 mL of ethanol by 2-min sonication. Both bead suspensions were then placed in 4-mL sealed amber vials, equipped with stir bars. PSC beads were functionalized with poly(2-vinylpyridine) before fluoresceinamine addition. A 0.5-mL aliquot of 0.4 M (monomer concentration) PVP in ethanol was added dropwise to the stirred PSC bead suspension, and the mixture was stirred for an additional 30 min. PVP was added first to ensure electrostatic binding of the positively charged PVP amines to carboxylate-functionalized PSC microbead surfaces prior to fluoresceinamine addition. Fluoresceinamine (0.5 mL, 10 mg/mL in ethanol) was then added dropwise to the PS microbead suspension and to the PSC microbeads coated with PVP. After 2 h of continuous stirring, both bead stocks were filtered with a conventional filtration setup equipped with a 25-mm diameter 0.45-μm pore size HVLP filter (Millipore) and washed with two 0.5-mL aliquots of 0.05 M phosphate buffer (pH 7.5). The microbeads were dried at 60 °C for 1 h.

Table 1. Vapor Pressure (VP) Data and Concentrations of the Compounds Used[a]

vapor	abbrev	VP (mmHg at 25 °C)	vapor concn (ppm) 50%	25%	10%
diisopropyl methylphosphonate	DIMP	0.3[b]	200	–	–
dimethyl methylphosphonate	DMMP	1.6[b]	1000	–	–
diethyl chlorophosphate	DCP	0.10[c]	66	33	13
methyl salicylate	MS	1.0[c,d]	660	–	–
ethanol	–	59[e]	39000	–	–
heptane	–	46[e]	30000	–	–
toluene	–	22[e]	14000	–	–
water	–	24[e]	16000	–	–

[a] Concentrations calculated in ppm correspond to saturated vapors mixed with air, and the content of the saturated vapor flow is expressed in %. [b] Obtained from ref 26. [c] Retrieved from the MSDS database. [d] T = 54 °C. [e] Obtained from ref 27.

Preparation of Microbead Arrays. Coverslip arrays and fiber bundle arrays were prepared as described previously.[19,20] Each vapor response was acquired with a new coverslip array, prepared by smearing a small portion of the microbead stock onto a glass coverslip.

Fluorescence Measurements. FLA solution (0.5 mM) was prepared by dissolving fluoresceinamine in 0.05 M phosphate buffer (pH 7.5). The 0.05 M phosphate buffer solutions with pH 3.1, 5.0, and 10.9 were prepared by adding concentrated HCl or NaOH to the pH 7.5 buffer to achieve the desired pH. The 0.5 mM solutions of FLPA were prepared by diluting a 10 mM ethanolic solution of FLPA with the four phosphate buffers. Fluorescence emission spectra were acquired with a microplate spectrofluorometer at 490-nm excitation and emission between 510 and 610 nm using a 5-nm wavelength step.

Solution Testing. A single-core optical fiber coupled to the imaging system was used to monitor the changes in fluorescence occurring when acryloyl chloride (AC), DCP, DIMP, and DMMP were added to the FLA solution. Excitation light (470 nm) was passed through the fiber, and the average emission intensity (550 nm) of a region on the proximal fiber end was measured with the CCD camera. The 370-μm-diameter single-core optical fiber used in the experiment was first polished using a series of lapping films (30, 12, 3, and 0.3 μm; Mark V Laboratories, East Granby, CT), rinsed with deionized water, and immersed into a 4-mL vial equipped with a stir bar. Two milliliters of 1 mM FLA solution was first pipetted into each vial, and 2, 3, 2, and 3 μL of AC, DIMP, DMMP, and DCP, respectively, were injected with a disposable syringe (Fisher Scientific) during constant stirring to achieve a ~10-fold stoichiometric amount of each reactant in solution. The first 20 data points were acquired in 1-s intervals. Each reagent was injected into the FLA solution immediately after the acquisition of the 10th data point. After the rapid data acquisition during the injection of the analytes in the beginning of the experiment, an additional 20 data points were acquired in 30-s intervals. The resulting overall experimental time was 620 s.

Collection of Vapor Responses. Vapor responses were acquired using coverslip arrays imaged by the fluorescence imaging system. The microbeads were excited at 470 nm, and their responses were monitored at 550-nm emission wavelength. Saturated vapors, mixed with ultra-zero-grade air to yield different vapor concentrations, were prepared with an automated vapor delivery system (GDS, Orono, ME) described in detail elsewhere.[20] In brief, saturated vapor of each analyte was prepared by passing air through liquid placed in a sealed bubbler. The desired concentrations of vapors were achieved by adjusting the percentages of saturated vapor and air flow rates, keeping the total flow at 200 mL/min (Table 1). The vapor delivery lines were purged with each vapor mixture for 45 s before the vapor was delivered to the array. The concentration of the headspace vapor was held constant by keeping the bubblers at 25 °C.

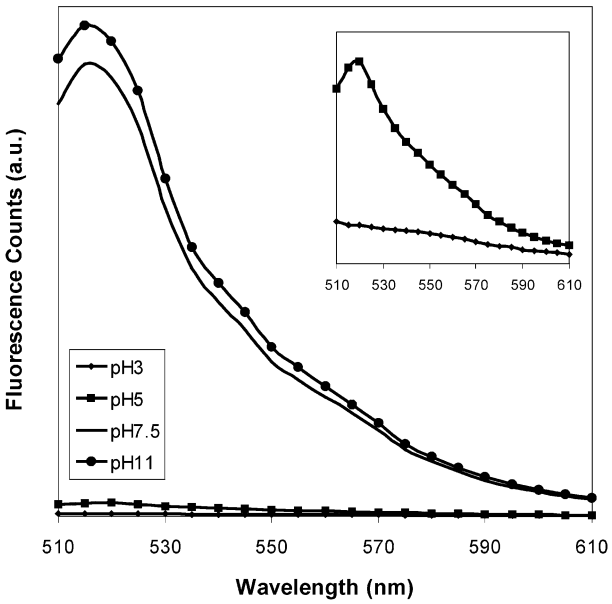

Figure 2. Emission spectra of 0.5 mM FLPA in 0.05 M phosphate buffers with pH values 3.1, 5.0, 7.6, and 10.9 (λ excitation = 490 nm). The inset shows expanded emission spectra of the product in pH 3.1 and pH 5.0 buffers.

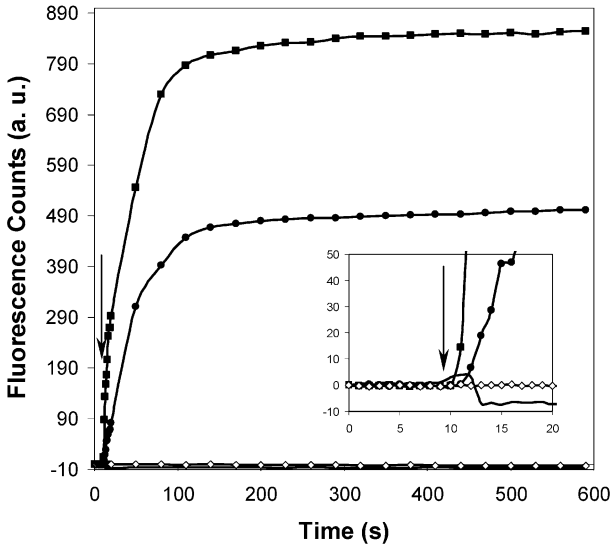

Figure 3. Baseline-subtracted fluorescence emission of 1 mM FLA (in 0.05 M phosphate pH 7.5 buffer), monitored over time, after addition of 10-fold stoichiometric amounts of AC (■), DCP (●), DIMP (no symbol), and DMMP (◇) (λ excitation = 470 nm, λ emission = 530 nm). The analytes were introduced 10 s after the beginning of data collection (see arrow in the inset plot).

Each 27-frame vapor response movie consisted of 17 100-ms fast-capture frames (two baseline frames, 10 frames collected during the vapor pulse, five frames collected after the pulse), and an additional 10 frames collected 30 s apart. The vapor pulse was 1.6 s long. After a vapor response had been acquired, the vapor delivery system lines were flushed with air for 2.5 min (200 mL/min), and a new coverslip array was positioned on the microscope before acquiring a new vapor response. The long purging of the vapor delivery tubing with air prevented any residues of previously used vapors from contaminating each newly prepared vapor mixture. For the 10 vapor sequences, a similar acquisition protocol was applied as for the individual vapor responses. After 12 100-ms exposures (two baseline frames, five pulse frames, and five frames following the pulse), 10 more frames were recorded in 15-s intervals. Each vapor pulse lasted 0.8 s. Once the 22 frames were acquired with the first vapor, the same data acquisition scheme was repeated for the next vapor and for each subsequent vapor in the sequence. The gas delivery lines were flushed with air for 10 min after each 10-vapor sequence. All vapor experiments were performed between 21 and 25 °C and between 21 and 50% relative humidity.

Results and Discussion

FLPA (Figure 1, III) was first synthesized and isolated to confirm the structure of the reaction product between FLA (I) and DCP (II). NMR characterization of the isolated product III validated the conversion to FLPA. According to ^{1}H NMR data, the FLPA 2′, 3′, and 5′ protons on the phenyl ring are deshielded relative to FLA protons (indicated in Figure 1). These downfield shifts result from the electron-withdrawing phosphoryl and correlate with the previously observed NMR downfield proton shifts of the amides derived from FLA.[25] In addition, the multiplet observed at 4.07 ppm indicates methylene splitting by both the methyl protons and the phosphorus. Once the irreversible reaction between FLA and DCP was confirmed, the reactivity of FLA was tested in solution with several phosphonates to observe the specificity of the reaction. Finally, we tested the interaction between the surface-immobilized indicator dye and DCP vapor using FLA-coated silica, polystyrene, and PVP-modified vinyl carboxylic acid/polystyrene copolymer microbeads.

Phosphoramide pH Dependence and Specificity. On the basis of previous interpretations,[25] FLA is quenched relative to its acyl derivative because the lone pair nitrogen of the amine group quenches the fluorescence via photoinduced electron transfer (PET). Upon reaction with an acyl or phosphoryl group, the amino group's lone pair is less available and increased fluorescence is observed. This increased fluorescence in FLPA is attributed to the withdrawal of electrons from the phenyl ring by the phosphoryl double-bonded oxygen. The electron density on the FLPA nitrogen and phenyl ring decreases, thereby reducing PET and increasing fluorescence. Fluorescein and most of its derivatives are known to exhibit strong pH dependence[25,28] as evidenced by the fact that fluorescein is a useful pH indicator. To verify pH sensitivity, fluorescence emission spectra of purified FLPA were acquired in different pH buffers and are shown in Figure 2. As can be seen in the figure, the fluorescence intensity of FLPA, observed at its emission maximum (λ_{max} = 515 nm), was significantly higher than FLA fluorescence and increased from pH 7.5 to pH 11, whereas the fluorescence intensities in acidic buffers (pH 3 and 5) were several orders of magnitude lower. These emission spectra confirm that FLPA exhibits the highest fluorescence at pH above neutral.

After optimizing the measurement pH, the turn-on behavior and FLA specificity for phosphoryl chloride were evaluated in solution. Four different reagents (AC, DCP, DIMP, and DMMP) were added to the FLA solution (pH 7.5), and the fluorescence intensity was measured over time. To perform these measurements in real time, a single-core optical fiber was immersed in the solution, and 10-fold stoichiometric amounts of AC, DCP,

(26) Taranenko, N.; Alarie, J.-P.; Stokes, D. L.; Vo-Dinh, T. *J. Raman Spectrosc.* **1996**, *27*, 379−384.
(27) Nelson, G. O. *Gas mixtures: preparation and control*; Lewis Publishers: Boca Raton, FL, 1992.
(28) Martin, M. M.; Lindqvist, L. *J. Lumin.* **1975**, *10*, 381−390.

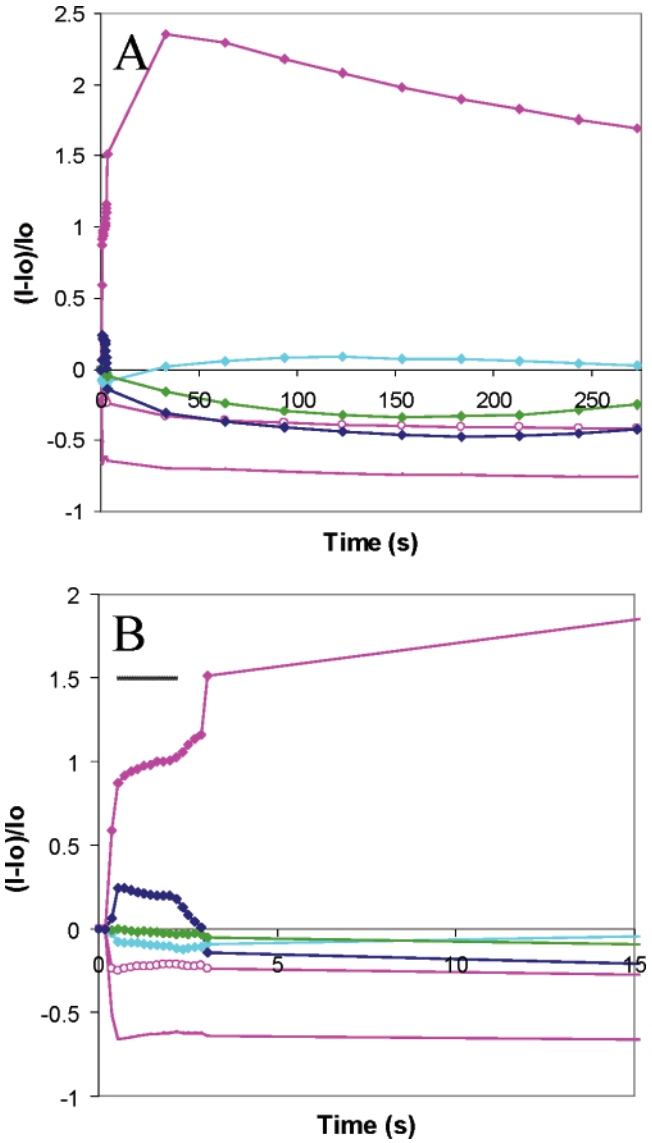

Figure 4. (A) Fluorescence responses of PSC/PVP/FLA (filled symbols), PS/FLA (open symbols), and S/FLA (no symbols) sensors during their exposure to 50% saturated DIMP (dark blue), DMMP (light blue), and DCP (magenta). The control response (green) was acquired with PSC/PVP/FLA microbeads exposed to ambient air. (B) Response shapes during the initial 15 s of acquisition (the duration of the pulse is indicated by the black bar).

DIMP, and DMMP were injected by syringe following an initial 10-s baseline acquisition. Figure 3 shows the fluorescence intensity of the solution, acquired through the optical fiber, during the various reactions. The inset shows the initial 30 s, indicating the time point when the reagents were injected. The additions of both AC and DCP resulted in increased fluorescence, which was attributed to amide and phosphoramide formation, respectively. The fluorescence due to the amide formation was greater in both rate and magnitude. These differences are likely due to the different reactivities of carbonyl and phosphoryl halides. In theory, carbonyl chlorides such as AC, which contain a highly electron-withdrawing alkenyl group adjacent to the carbonyl, should react much faster than phosphoryl chlorides which contain a weaker electron-withdrawing phosphoryl. Moreover, the higher reactivity of the sp^2 carbonyl arises also from the fact that the carbon is less sterically hindered than the highly coordinated phosphorus. Despite the lower change in intensity for the DCP reaction, the intensity increase

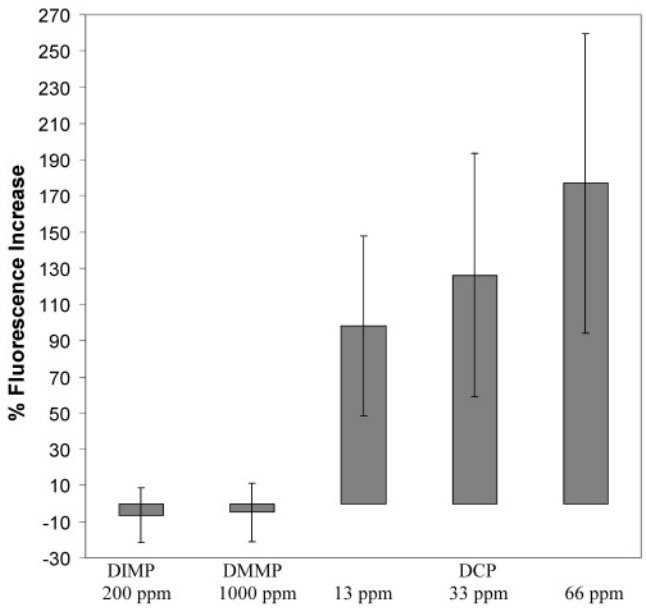

Figure 5. Fluorescence % increase recorded 33 s after the beginning of the 1.6-s pulse. The values represented are the calculated averages and standard deviations of 50 PSC/PVP/FLA microbeads per array, selected randomly from individual arrays ($N = 8$) and exposed to 200 ppm DIMP, 1000 ppm DMMP, or 13, 33, and 66 ppm DCP.

confirmed the predicted turn-on behavior resulting from FLA derivatization with DCP. FLA specificity toward DCP was confirmed by monitoring the fluorescence of FLA mixed with nonreactive phosphonates (DIMP and DMMP). These reaction mixtures did not exhibit a fluorescence change over time, indicating that these two simulants did not react with FLA.

These solution-based experiments demonstrated the specificity of FLA for phosphoryl halides and the intense fluorescence of the resulting phosphoramide. In solution, the fluorescence increase obtained was due to careful pH control. These results were considered in the preparation of vapor-sensitive FLA-coated microbeads with turn-on behavior.

Responses of FLA-Coated Microbeads to DCP. The HCl that forms as a byproduct of the reaction between FLA and DCP could potentially cause a local decrease in pH, thereby quenching the FLPA adduct. By buffering the solution, HCl is neutralized. Maintaining the proper pH is more challenging when the reaction occurs in the solid state. With a solid phase reaction on microbeads, a proton sponge is required to maintain the microenvironment pH at a value where the FLPA remains highly fluorescent. FLPA quenching on the surface due to HCl was circumvented by preparing microbeads with surface groups that could neutralize the acid byproduct. To determine which microbead type would work best, FLA was adsorbed onto three different types of microbeads: silica (S), polystyrene (PS), and carboxylate-functionalized polystyrene (PSC). Surfaces of the first two microbead types were not modified, whereas the third microbead type was coated with a layer of PVP. We chose PVP due to its basicity (conjugate acid $pK_a \approx 4$).[29] The PVP proton-accepting groups were expected to prevent acidification of FLPA. The surfaces of all three bead types were rinsed in buffer (pH 7.5) to convert FLA into its basic form and deprotonate the hydroxyl groups on silica bead surfaces,[30] any remaining carboxyl groups on PSC bead surfaces, and PVP moieties.[29]

(29) Ripoll, C.; Muller, G.; Selegny, E. *Eur. Polym. J.* **1971**, *7*, 1393−1409.
(30) Tao, Z.; Zhang, H. *J. Colloid Interface Sci.* **2002**, *252*, 15−20.

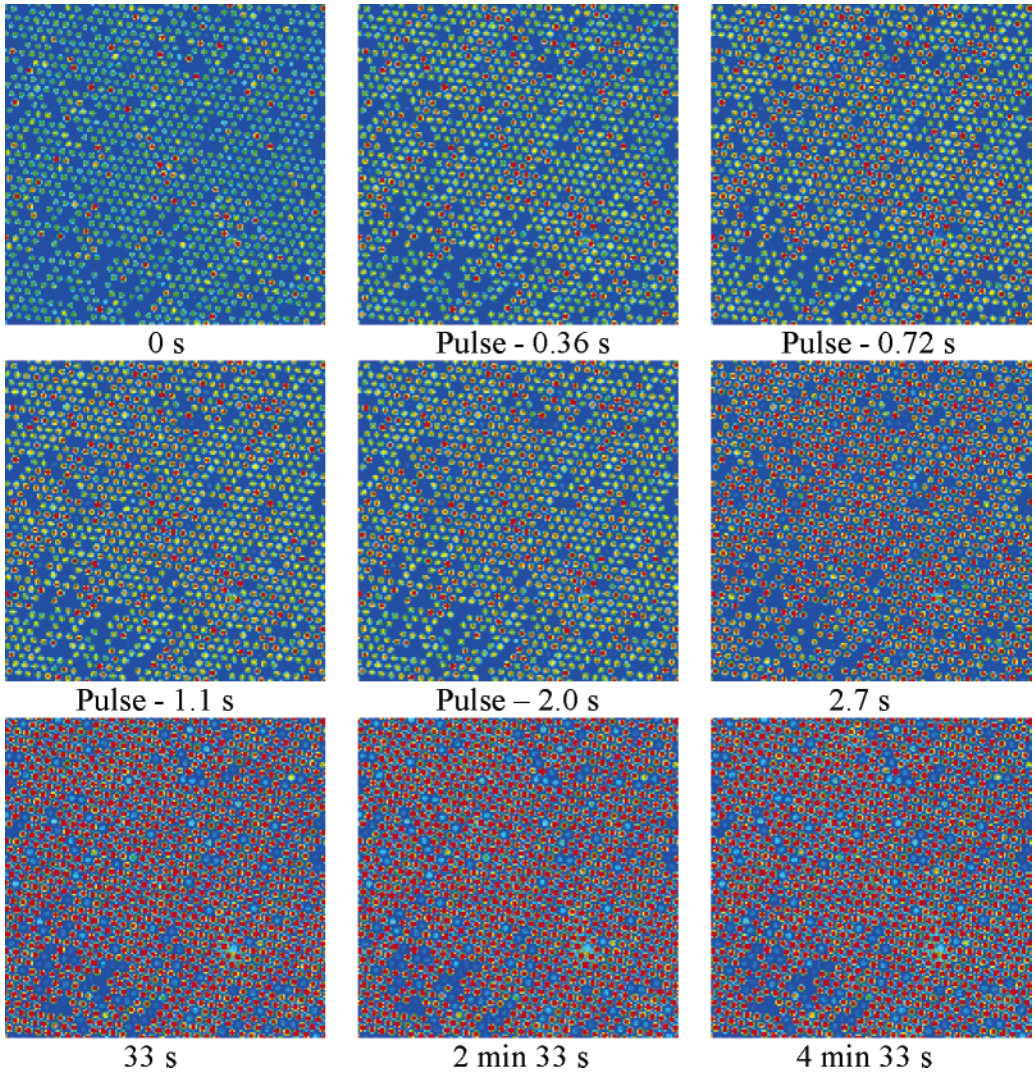

Figure 6. Sequential images of an array of 4.5-μm wells filled with PSC/PVP/FLA microbeads that turn on irreversibly during and after a 1.6-s pulse of 66 ppm DCP vapor.

DCP vapor responses of the three microbead types (S/FLA, PS/FLA, and PSC/PVP/FLA) were acquired to determine which type would respond most rapidly and with the highest irreversible fluorescence increase. Each vapor response was acquired with a freshly prepared coverslip array, positioned on the optical microscope. The delivery of the vapors and the sequence in which the different microbead types were tested were randomized. DCP vapor responses of the three microbead types are shown in magenta in Figure 4. Whereas S/FLA (no symbols) and PS/FLA (circles) microbeads did not turn on during exposure to 66 ppm DCP, the PSC/PVP/FLA microbeads (filled circles) exhibited a dramatic fluorescence increase. The fluorescence intensity increase was highest (more than 200% increase) approximately 33 s after the vapor pulse, and although it decreased slightly over time, the increase was larger than 150% even 4 min after vapor exposure. The largest fluorescence increase occurred after the pulse was discontinued. The increase in intensity during and after the vapor pulse (Figure 4 B) suggests that FLPA formed on the surface of the beads and the PVP layer effectively neutralized the acid produced. The fluorescence of the S/FLA and PS/FLA microbeads decreased dramatically at the beginning of the DCP pulse and only slightly increased during the remainder of the exposure (Figure 4B). The overall fluorescence was quenched after vapor exposure. This observation can be attributed to the buildup of HCl on the surface of the microbeads. Moreover, strong hydrogen bonding between the organophosphate molecules and hydroxyl groups on the silica surface likely occurred,[31] which may have caused surface saturation with DCP and prevented the microbead surface from returning to its initial condition and the dye from returning to its unbleached state.

In addition to DCP vapor, the PSC/PVP/FLA microbeads were exposed to nonreactive control vapors to confirm the specificity of the reaction between surface-bound FLA and vapor-phase DCP. The array was exposed to either 200 ppm DIMP (light blue) or 1000 ppm DMMP (dark blue, Figure 4). As expected, the microbeads exposed to unreactive vapors did not turn on and their fluorescence changed only slightly over time. An air exposure was used as an additional control to determine whether the small change in fluorescence intensity over time originated from photobleaching. Although the fluorescence intensity of the array exposed to ambient air (shown in green in Figure 4) decreased somewhat over time, the decrease may have been due to changes in relative humidity

(31) Kanan, S. M.; Tripp, C. P. *Langmuir* **2001**, *17*, 2213−2218.

surrounding the microbead probes, in addition to any photobleaching. Humidity effects will be discussed in more detail below.

Sensitivity and Microarray Response of PSC/PVP/FLA Microbeads. The sensitivity of the PSC/PVP/FLA microbeads was tested by exposing freshly prepared arrays to three different concentrations of DCP. Fifty percent saturated DIMP and DMMP vapors were used as controls. Figure 5 shows the % increase in fluorescence intensities of coverslip arrays containing approximately 50 beads. The fluorescence intensity values in the plot were measured 33 s after the beginning of a 1.6-s vapor pulse. Each of the five averaged intensities (13, 33, and 66 ppm DCP, 200 ppm DIMP, and 1000 ppm DMMP) was calculated using data from eight different arrays per vapor type, as each array was exposed only once to an individual vapor pulse because of the irreversible reaction. The intensities of microbeads exposed to DIMP and DMMP remained within baseline values, and as expected, microbead intensities increased with increasing DCP vapor concentration. Standard deviations of the three DCP averages were high (47−53%), likely because each response was acquired with a different array. Despite the careful preparation of the microbeads coated with polymer and dye, the ability to control PVP and FLA adsorption on the bead surfaces was limited, thereby causing some nonhomogeneous surface coverage and lower bead-to-bead reproducibility. As these probes are designed more for alerting to the presence/absence of a harmful vapor exposure, quantitative measurements are less important than a measurable response.

To further demonstrate the feasibility of the PSC/PVP/FLA probes for use in array-based systems, the microbeads were positioned onto an array of microwells etched into an optical fiber bundle. A series of CCD images, shown in Figure 6, show the progression of a microbead array response to 66 ppm DCP vapor. The array contains one microbead per well. The bead intensities are low at the beginning of the experiment and gradually increase during the vapor pulse (0.36−2.0 s), as shown by the increasing red color in the images. As observed in the time plots shown in Figure 4, the fluorescence in this experiment also continues to increase after the pulse and remains high throughout the monitoring period.

Having the capability to include single-use microbeads in a high-density microbead array is of utmost importance, as the presence of reactive substances such as DCP could potentially destroy the sensitivity of other cross-reactive sensors. In such cases, turn-on FLA probes would be the only microbeads in the array that would indicate a problem.

Multivapor Sequences. After demonstrating both the turn-on behavior of the PSC/PVP/FLA probes and their irreversibility upon vapor exposure, it was important to show that these microbeads could be used for real-time monitoring. Monitoring was performed by observing continuous microbead responses to 10-vapor sequences, during which the microbead fluorescence was expected to increase only in the presence of DCP and remain unchanged in the presence of all other vapors. The classes of 50% saturated vapors included nerve agent simulants (DCP, DMMP, and DIMP), a mustard gas simulant (methyl salicylate), common volatile organic vapors (ethanol, heptane, and toluene), water, and air. These vapors, listed in Table 1, were selected such that they were at least an order of magnitude higher than the DCP concentration. Since our preliminary

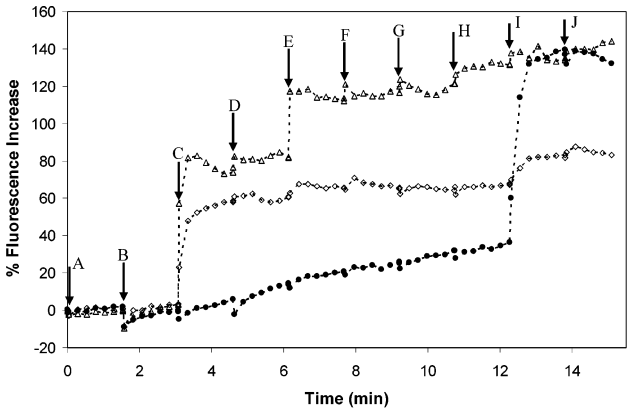

Sequence	A	B	C	D	E	F	G	H	I	J
•	air	DMMP	toluene	ethanol	heptane	water	air	MS	DCP	air
Δ	air	DMMP	DCP	air	DCP	heptane	toluene	air	water	air
◊	air	DMMP	DCP	toluene	water	heptane	MS	air	DCP	air

Figure 7. Averaged responses of 50 PSC/PVP/FLA sensor microspheres exposed to three different series of 50% saturated vapors. Each vapor was pulsed to the sensor array for 0.8 s, and the resulting change of fluorescence intensity was recorded in 15-s intervals. The arrows indicate the beginning of each vapor pulse and correspond to the randomized vapor sequences (A−J) summarized in the corresponding table below the plot. DMMP, dimethyl methylphosphonate; DCP, diethyl chlorophosphate; MS, methyl salicylate.

experiments described above with PSC/PVP/FLA microbeads indicated that humidity changes slightly affected the fluorescence intensity, the vapor pulse duration in this experiment was shortened. The resulting simulated real-time monitoring experiment involved 0.8-s vapor pulses delivered to the microbeads in preprogrammed sequences of the 10 vapors. The microbead fluorescence was measured during and up to ∼1.5 min after each subsecond vapor pulse. Figure 7 shows three examples of microbead responses that were recorded with three different 10-vapor sequences. The table under the figure contains the sequence information of vapors, letter coded A−J in the plot, which coincide with the delivery points indicated by arrows. In all the sequences, DCP pulses were the only ones that resulted in a sharp and stable fluorescence increase. In all three monitoring sequences, the fluorescence intensity had increased to between 44 and 79% 16 s after the first DCP vapor pulse and remained almost as high more than a minute later. Whenever a second DCP pulse was applied (sequences marked by triangles and diamonds in Figure 7), the fluorescence increase was significantly smaller than the first increase, suggesting that most FLA molecules on the microbead surface had already reacted with DCP during the first pulse. None of the other vapors changed the microbead fluorescence intensities; however, the fluorescence gradually drifted to higher intensity values over time (e.g., filled circles in Figure 7). The baseline fluorescence decreased or increased slightly during many additional control experiments (not shown here), similar to the control response acquired with microbeads exposed to air (shown in green, Figure 4). Since the pulses were extremely short and because the array exposure to light was minimized during these experiments, the random and small changes in baseline intensity over time are probably a consequence of variable humidity in the microbead environment. Despite the gradual baseline drift, the rapid fluorescence increase and distinct response shapes allow easy identification of DCP vapor exposure, thereby indicating specificity for real-time chemical warfare agent monitoring. It is important to note that although these probes do not respond

to nonreactive phosphonates and additional VOCs, they will respond to other reactive compounds such as acyl halides and acetic anhydrides as described in our previous work.[25] While this lack of specificity toward reactive organophosphates may be viewed as a limitation, these other reactive and toxic substances are not supposed to be present in the environment and it would be important to detect them as well. If acyl halides and acetic anhydrides were released into the ambient environment, the sensors would provide a fluorescence increase that would indicate the presence of these other harmful vapors. Such false positives would still trigger a necessary evacuation.

Conclusion

In this article, we described microbead probes that turn on when exposed to reactive vapors. The microbeads, coated with fluoresceinamine and poly(2-vinylpyridine), have subsecond response times when exposed to 13 ppm vapors of the nerve agent simulant DCP. The irreversible conversion of FLA to a phosphoramide provides selectivity across many classes of vapors including nonreactive nerve simulants and a mustard warfare simulant, as the increased fluorescence remained unchanged after exposure to DCP. Because these microbeads respond selectively and irreversibly, their responses do not require further data analysis, which makes them ideal for rapid detection of harmful vapors. The reactivity toward DCP was maintained even after the microbeads were exposed to multiple nonreactive vapors. On the basis of these results, the inclusion of such microbeads in a microarray may enable confirmation of chemical warfare release within a few seconds. Although these microbeads were tested only with DCP vapor, the reactivity of FLA suggests their applicability for a number of nerve agents and other harmful reactive vapors.

Acknowledgment. This work was funded in part by DARPA. We thank Viatcheslav Azev for MS characterization and helpful discussions.

JA057057B